

Dynamic Risk Prediction Using Survival Tree Ensembles with Application to Cystic Fibrosis

Yifei Sun, Sy Han Chiou, Colin O. Wu, Meghan McGarry, and Chiung-Yu Huang

Abstract

With the availability of massive amounts of data from electronic health records and registry databases, incorporating time-varying patient information to improve risk prediction has attracted great attention. To exploit the growing amount of predictor information over time, we develop a unified framework for landmark prediction using survival tree ensembles, where an updated prediction can be performed when new information becomes available. Compared to the conventional landmark prediction, our framework enjoys great flexibility in that the landmark times can be subject-specific and triggered by an intermediate clinical event. Moreover, the nonparametric approach circumvents the thorny issue in model incompatibility at different landmark times. When both the longitudinal predictors and the outcome event time are subject to right censoring, existing tree-based approaches cannot be directly applied. To tackle the analytical challenges, we consider a risk-set-based ensemble procedure by averaging martingale estimating equations from individual trees. Extensive simulation studies are conducted to evaluate the performance of our methods. The methods are applied to the Cystic Fibrosis Patient Registry (CFFPR) data to perform dynamic prediction of lung disease in cystic fibrosis patients and to identify important prognosis factors.

KEY WORDS: Dynamic prediction, landmark analysis, multi-state model, survival tree, time-dependent predictors.

Yifei Sun is Assistant Professor, Department of Biostatistics, Columbia University Mailman School of Public Health, New York, NY 10032 (Email: ys3072@cumc.columbia.edu). Sy Han Chiou is Assistant Professor, Department of Mathematical Sciences, University of Texas at Dallas (Email: schiou@utdallas.edu). Meghan McGarry is Assistant Professor, Department of Pediatrics, School of Medicine, University of California San Francisco (Email: [Meghan.McGarry@ucsf.edu](mailto: Meghan.McGarry@ucsf.edu)). Colin O. Wu is Mathematical Statistician, National Heart, Lung, and Blood Institute, National Institutes of Health (Email: wuc@nhlbi.nih.gov). Chiung-Yu Huang is Professor, Department of Epidemiology and Biostatistics, School of Medicine, University of California San Francisco, San Francisco, CA 94158 (Email: ChiungYu.Huang@ucsf.edu).

1 Introduction

Cystic fibrosis (CF) is a genetic disease characterized by a progressive, irreversible decline in lung function caused by chronic microbial infections of the airways. Despite recent advances in diagnosis and treatment, the burden of CF care remains high, and most patients succumb to respiratory failure. There is currently no cure for CF, so early intervention and prevention of lung disease for high-risk patients are essential for successful disease management. The goal of this research is to develop flexible and accurate risk prediction algorithms for abnormal lung function in pediatric CF patients by exploiting the rich longitudinal information made available by the Cystic Fibrosis Foundation Patient Registry (CFFPR).

The CFFPR is a large EHR database that collects encounter-based records of over 300 unique variables on patients from over 120 accredited CF care centers in the United States (Knapp et al., 2016). The CFFPR contains detailed information on potential risk factors for abnormal lung function, including symptoms, pulmonary infections, medications, test results, and medical history. Analyses of CFFPR suggested that the variability in spirometry measurements over time is highly predictive of subsequent lung function decline (Morgan et al., 2016). Moreover, the acquisition of chronic, mucoid, or multidrug-resistant subtypes of *Pseudomonas aeruginosa* (PA) often leads to more severe pulmonary disease, accelerating the decline in pulmonary function (McGarry et al., 2020). In this paper, the event of interest is the progressive loss of lung function, defined as the first time that the predicted forced expiratory volume in 1 second (ppFEV1) drops below 80% in CFFPR. Since risk factors such as weight and height in pediatric CF patients can change substantially over time, models with only baseline variables have limited potential for long-term prognosis. Incorporating longitudinal measurements and intermediate clinical events would reflect ongoing CF management and growth trajectory better than using a single baseline measurement, and thus results in more accurate prediction. The goal of this research is to develop prediction algorithms that can fully utilize the accumulating history information.

To incorporate the longitudinal patient information in risk prediction, one major approach is joint modeling (see, for example, Rizopoulos, 2011; Taylor et al., 2013). Under the joint modeling framework, a longitudinal submodel for the time-dependent variables and a survival submodel for the time-to-event outcome are postulated, where the sub-models are typically linked via shared latent variables. Such a model formulation provides a complete specification of the joint distribu-

tion, based on which the survival probability given the history of longitudinal measurements can be derived. Most joint modeling methods consider a single, continuous time-dependent variable. Although attempts have been made to incorporate multiple time-dependent predictor variables (Proust-Lima et al., 2016; Wang et al., 2017), correct specification of the model forms for all the time-dependent covariates and their associations with the event outcome remains a major challenge. Moreover, it is not clear how existing joint modeling approaches can further incorporate the information on the multiple intermediate events, such as the acquisition of different subtypes of PA, in risk prediction.

Another major approach that can account for longitudinal predictors is landmark analysis, where models are constructed at pre-specified landmark times to predict the event risk in a future time interval. For example, at each landmark time, one may postulate a working Cox model with appropriate summaries of the covariate history up to the landmark time as predictors and then fit the Cox model using data from subjects who are at risk of the event (see van Houwelingen, 2007; van Houwelingen and Putter, 2008, 2011). In this way, multiple and mixed type time-dependent predictors can be easily incorporated. Other than the standard Cox models, Parast et al. (2012) considered time-varying coefficient models to incorporate a single intermediate event and multiple biomarker measurements. Zheng and Heagerty (2005) and Zhu et al. (2019) further considered the impact of informative observation times of repeated measurements on future risk.

Direct application of the existing landmark analysis method to the CFFPR data is not ideal for the following reasons: first, fitting semiparametric working models separately at different landmark times may result in incompatible models and inconsistent predictions (Jewell and Nielsen, 1993; Rizopoulos et al., 2017; Li et al., 2017). In other words, a joint distribution of predictors and event times that satisfies all the models imposed at the landmark times simultaneously may not exist. Second, the specification of how the history of predictors affects the risk of events may require deep clinical insight. For example, researchers have shown that various summaries of the repeated measurements, including the variability (Morgan et al., 2016; Vidal-Petiot et al., 2017), the rate of change (Mannino et al., 2006), and the area under the trajectory curve (Domanski et al., 2020), can serve as important predictors of disease risks. To this end, nonparametric statistical learning methods are appealing in landmark prediction, because they require minimal model assumptions and have the potential to deal with a large number of complicated predictors.

In this paper, we propose a unified framework for landmark prediction using survival tree en-

sembles, where the landmark times can be fixed or subject-specific. A subject-specific landmark can be defined by an intermediate clinical event that modifies patients’ risk profiles and triggers the need for an updated evaluation of future risk. In our application, the acquisition of chronic PA usually leads to accelerated deterioration in the pulmonary function and serves as a natural landmark. When the landmark time is random, the number of observed predictors at the landmark time often varies across subjects, creating analytical challenges in fully utilizing the available information. Moreover, unlike static risk prediction models where baseline predictors are completely observed, the observation of the time-dependent predictors is further subject to right censoring. To tackle these problems, we propose a risk-set-based approach to handle the possibly censored predictors. To avoid the instability issue of a single tree, we propose a novel ensemble procedure based on averaging unbiased martingale estimating equations derived from individual trees. Our ensemble method is different from existing ensemble methods that directly average the cumulative hazard predictions and has strong empirical performances in dealing with censored data.

The rest of this article is organized as follows. In Section 2, we introduce a landmark prediction framework that incorporates the repeated measurements and intermediate events. In Section 3, we propose tree-based ensemble methods to deal with censored predictors and outcomes. We propose a concordance measure to evaluate the prediction performance in Section 4 and define a permutation variable importance measure based on the out-of-bag concordance in Section 5. The proposed methods are evaluated by extensive simulation studies in Section 6 and are applied to the CFFPR data in Section 7. We conclude the paper with a discussion in Section 8.

2 Model Setup

In contrast to conventional static risk prediction methods that output a conditional survival function given baseline predictors, dynamic landmark prediction focuses on the survival function conditioning on the predictor history up to the landmark time. Since history information usually involves complicated stochastic processes, challenges arise as to how to partition the history processes when applying tree-based methods. In what follows, we first introduce a generalized definition of the landmark survival function, starting from either a fixed or subject-specific landmark time. We then express the history information as a fixed-length predictor vector on which recursive partition can be applied.

Denote by T a continuous failure event time and by T_L a landmark time. In this paper, we allow T_L to be either fixed or subject-specific. We focus on the subpopulation that is free of the failure event at T_L and predict the risk after T_L . Denote by \mathbf{Z} the baseline predictors and denote by $\mathcal{H}(t)$ other information observed on $[0, t]$. Our goal is to predict the probability conditioning on all the available information up to T_L , that is,

$$P(T - T_L \geq t \mid T \geq T_L, T_L, \mathcal{H}(T_L), \mathbf{Z}). \quad (2.1)$$

To illustrate the observed history $\mathcal{H}(t)$, we consider two types of predictors that are available in the CFFPR database. The first type of predictors is repeated measurements of time-dependent variables such as weight and ppFEV1. We denote this type of predictors by $\mathbf{W}(t)$, a q -dimensional vector of time-dependent variables, and assume $\mathbf{W}(\cdot)$ is available at fixed time points t_1, t_2, \dots, t_K . The observed history up to t is $\mathcal{H}_W(t) = \{\mathbf{W}(s)dO(s), 0 < s \leq t\}$, where $O(t)$ is a counting process that jumps by one when $\mathbf{W}(\cdot)$ is measured (i.e., $dO(t_k) = 1$ for $k = 1, \dots, K$). The second type of predictors are the timings of intermediate clinical events such as pseudomonas infections. Denote by U_j the time to the j th intermediate event, $j = 1, \dots, J$. The observed history up to t is $\mathcal{H}_U(t) = \{I(U_j \leq s), 0 < s \leq t, j = 1, \dots, J\}$. Collectively, we have a system of history processes $\mathcal{H}(t) = (\mathcal{H}_W(t), \mathcal{H}_U(t))$.

In our framework, both t_k and U_j can serve as landmark times. Due to the stochastic nature of U_j , the order of $\{t_k, U_j, k = 1, \dots, K, j = 1, \dots, J\}$ can not be pre-determined. As a result, the number of available predictors at a given landmark time can vary across subjects. For illustration, we consider one fixed time point t_1 at age 7 and one intermediate event chronic PA (cPA), of which the occurrence time is denoted by U_1 . Figure 1 depicts the observed data of two study subjects. At $t_1 = 7$, subject 1 has experienced cPA ($U_1 = 4.8 \leq t_1$), while subject 2 remains free of cPA ($U_1 = 10.2 > t_1$). Let $\mathbf{W}(t)$ be the body weight measured at time t (i.e., $q = 1$). The probabilities of interest are given as follows:

- (I) At a fixed landmark time $T_L = t_1$, we predict the risk at $t_1 + t$, $t > 0$, among those who are at risk, that is, $T \geq t_1$. Note that subjects in the risk set may or may not have experienced the intermediate event prior to t_1 . Given $\mathbf{W}(t_1)$ and the partially observed U_1 , the conditional

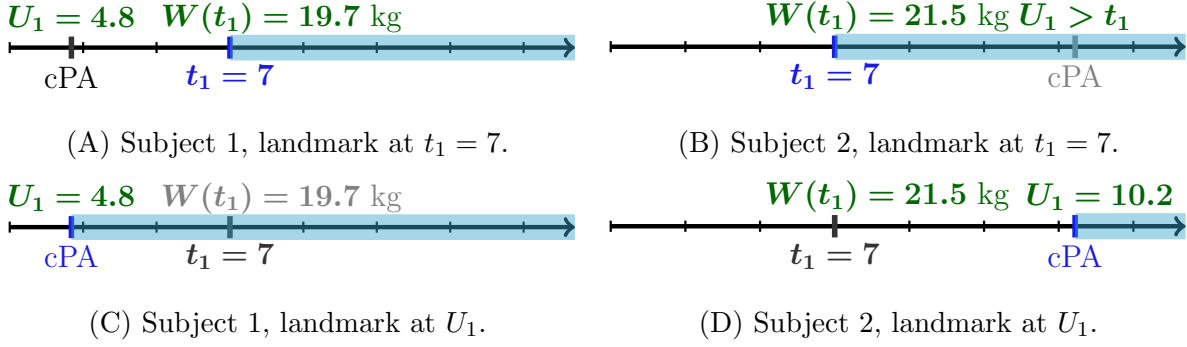


Figure 1: Illustration of fixed and random landmark times. \blacksquare marks the landmark time point; \blacksquare marks the available information at the landmark time; \blacksquare marks the unavailable information at the landmark time; \blacksquare marks the target prediction interval.

survival probability (2.1) can be reexpressed as

$$\begin{cases} P(T \geq t + t_1 \mid T \geq t_1, \mathbf{Z}, \mathbf{W}(t_1), U_1), & \text{if } U_1 \leq t_1, \\ P(T \geq t + t_1 \mid T \geq t_1, \mathbf{Z}, \mathbf{W}(t_1), U_1 > t_1), & \text{otherwise.} \end{cases}$$

In other words, at t_1 , we output the former for subjects who experience the intermediate event prior to t_1 (subject 1, Figure 1A), while output the latter for others (subject 2, Figure 1B).

- (II) At a random landmark time $T_L = U_1$, we predict the risk for subjects who have experienced the intermediate event and are free of the failure event. The predictor value $\mathbf{W}(t_1)$ is available only if $U_1 \geq t_1$. In this case, we predict

$$\begin{cases} P(T \geq t + U_1 \mid T \geq U_1, \mathbf{Z}, U_1), & \text{if } U_1 \leq t_1, \\ P(T \geq t + U_1 \mid T \geq U_1, \mathbf{Z}, \mathbf{W}(t_1), U_1), & \text{otherwise.} \end{cases}$$

Therefore, at U_1 , we output the former for subjects whose $\mathbf{W}(t_1)$ is observed after U_1 (subject 1, Figure 1C), while output the latter for others (subject 2, Figure 1D).

In the above example, the observed predictors may vary across subjects. In what follows, we represent the history $\mathcal{H}(T_L)$ as a vector with a fixed length, so that tree-based methods can be applied to estimate probability (2.1). Define the complete predictors $\mathbf{X} = \{\mathbf{W}(t_1), \dots, \mathbf{W}(t_K), U_1, \dots, U_J\}$. The information in \mathbf{X} may not be fully available at a given landmark time, while more information become available at later landmark times. We define the available information up to t by

$\mathbf{X}(t) = \{\mathbf{W}(t_1, t), \dots, \mathbf{W}(t_K, t), U_1(t), \dots, U_J(t)\}$, where

$$\mathbf{W}(t_k, t) = \begin{cases} \mathbf{W}(t_k), & \text{if } t_k \leq t, \\ \mathbf{NA}_q, & \text{otherwise,} \end{cases} \quad U_j(t) = \begin{cases} U_j, & \text{if } U_j \leq t, \\ t^+, & \text{otherwise.} \end{cases}$$

With slight abuse of notation, we write $U_j(t) = t^+$ if and only if $U_j > t$, and write $\mathbf{W}(t_k, t) = \mathbf{NA}_q$ if and only if $\mathbf{W}(t_k)$ is not available at t (i.e., $t_k > t$), with $\mathbf{NA}_q \stackrel{\text{def}}{=} (\text{NA}, \dots, \text{NA})$ denoting a non-numeric q -dimensional vector. In this way, the history $\mathcal{H}(T_L)$ can be represented by $\mathbf{X}(T_L)$, which is a $(qK + J)$ -dimensional vector. Then the target probability function can be expressed in the following form,

$$S(t \mid a, \mathbf{z}, \mathbf{x}) = P(T \geq t + a \mid T \geq T_L = a, \mathbf{Z} = \mathbf{z}, \mathbf{X}(T_L) = \mathbf{x}). \quad (2.2)$$

In the examples depicted in Figure 1, we have $\mathbf{X}(t) = \{\mathbf{W}(t_1, t), U_1(t)\}$. For $T_L = t_1$, the predictor values in Figure 1A and Figure 1B correspond to $\mathbf{x} = (19.7, 4.8)$ and $\mathbf{x} = (21.5, 7^+)$, respectively. For $T_L = U_1$, the predictor values in Figure 1C and Figure 1D correspond to $\mathbf{x} = (\text{NA}, 4.8)$ and $\mathbf{x} = (21.5, 10.2)$, respectively.

Since the information available at T_L involves left-bounded intervals and non-numeric values, it is difficult to apply semiparametric methods such as Cox-type models to estimate $S(t \mid a, \mathbf{z}, \mathbf{x})$. In Section 3, we propose partition-based estimation to handle the partially observed predictors.

3 Survival trees and ensembles for landmark prediction

At a given landmark time, we build a tree-based model to predict future event risk. Survival trees have been popular nonparametric tools for risk prediction (Zhang and Singer, 2010). The original survival trees usually take the baseline predictors as the input variables and output the event free probability conditioning on the baseline predictors (see, for example, Gordon and Olshen, 1985; Ciampi et al., 1986; Segal, 1988; Davis and Anderson, 1989; LeBlanc and Crowley, 1992, 1993; Zhang, 1995; Molinaro et al., 2004; Steingrimsson et al., 2016), and ensemble methods have been commonly applied to address the instability issue of a single tree (Hothorn et al., 2004, 2006; Ishwaran et al., 2008; Zhu and Kosorok, 2012; Steingrimsson et al., 2019). However, existing methods may not be directly applied, because the predictors in \mathbf{X} are not completely observed at T_L and the available predictors in $(T_L, \mathbf{X}(T_L))$ are further subject to right censoring. In the absence

of censoring, we introduce a partition scheme for subjects who are event-free at the landmark time in Section 3.1. In Section 3.2, we propose risk-set methods to estimate the partition-based landmark survival probability. In Section 3.3, we propose an ensemble procedure that averages partition-based estimating equations to improve the prediction performance.

3.1 Partition on partially observed predictors at the landmark time

A tree partitions the predictor space into disjoint subsets termed terminal nodes and assigns the same survival prediction for subjects that enter the same terminal node. In dynamic risk prediction, the population of interest is subjects who remain event-free at the landmark time, that is, those with $T \geq T_L$. We use $\mathcal{T} = \{\tau_1, \tau_2, \dots, \tau_M\}$ to denote a partition on the sample space of $(T_L, \mathbf{Z}, \mathbf{X}(T_L)) \mid T \geq T_L$, where $\tau_m, m = 1, \dots, M$, are the terminal nodes. The terminal nodes are formed recursively using binary partitions by asking a sequence of yes-or-no questions. When a variable is numeric, existing approaches usually consider axis-parallel partition rules of the form “Is the variable $> c$?” for a cutoff value c . Since $\mathbf{X}(T_L)$ involves non-numeric features, the conventional partition scheme needs to be extended.

When the landmark time T_L is fixed at a with $t_m \leq a < t_{m+1}$, the candidate splitting variables are $\{\mathbf{Z}, \mathbf{W}(t_1, a), \dots, \mathbf{W}(t_m, a), U_1(a), \dots, U_J(a)\}$. For $k = 1, \dots, m$, we have $\mathbf{W}(t_k, a) = \mathbf{W}(t_k)$, and thus splitting based on variables in $\mathbf{W}(t_k, a)$ are straightforward. For splitting based on $U_j(a)$, the cut-off value c cannot exceed a , because $U_j(a) = a^+$ is considered as an attribute. When $c = a$, subjects who have not experienced the j th intermediate event before or at a enter the same child node, regardless of their actual values of U_j .

When T_L is random, the partition is based on the variables in $(T_L, \mathbf{Z}, \mathbf{X}(T_L))$. We consider the following situations:

- (R1) When $\mathbf{W}(t_k, T_L)$'s are used as splitting variables, the axis-parallel partition rule cannot be directly applied as they take NA values when $t_k > T_L$. Given a cutoff value c on a variable W in $\mathbf{W}(t_k, T_L)$, the node memberships of individuals with $t_k \leq T_L$ can be easily determined based on the rule “Is $W > c$?”. Individuals with $t_k > T_L$ have $W = \text{NA}$ and can be assigned to either the left or right child node. Specifically, one can split the data based on W and a cut off value c using one of the two options: (a) “Is $W > c$ and $t_k \leq T_L$?”, i.e., subjects with $W \leq c$ or $W = \text{NA}$ are classified in the same child node; (b) “Is $W > c$ or $t_k > T_L$?”,

i.e., subjects with $W > c$ or $W = \text{NA}$ are classified in the same child node. It is worthwhile to point out that $W = \text{NA}$ is treated as an attribute rather than missing data, because the target probability when $T_L < t_k$ is not conditioning on the actual value of W . On the other hand, implementing such a partition rule is equivalent to the “missings together” approach (Zhang et al., 1996) in dealing with missing data in predictors.

(R2) When $U_j(T_L)$ is used as a splitting variable, the axis-parallel partition rule $U_j(T_L) > c$ cannot be directly applied because the value T_L^+ is ambiguous for partitioning. To tackle this problem, we use a transformed set of predictors on intermediate events, $\{U_j(T_L)/T_L, \dots, U_J(T_L)/T_L\}$, which, together with T_L , contains the same information as $\{U_j(T_L), \dots, U_J(T_L), T_L\}$. Then the axis-parallel rule $U_j(T_L)/T_L > c$ can be applied for $c \in (0, 1]$, and $U_j(T_L)/T_L > 1$ is equivalent to $U_j(T_L) = T_L^+$.

The partition scheme described above guarantees that each individual has a well-defined pathway to determine its node membership. Given such a partition \mathcal{T} , one can define a partition function $l_{\mathcal{T}}(a, \mathbf{z}, \mathbf{x})$, which returns the terminal node in \mathcal{T} that contains $(a, \mathbf{z}, \mathbf{x})$. We define the following partition-based survival function,

$$S_{\mathcal{T}}(t \mid a, \mathbf{z}, \mathbf{x}) = P(T \geq t + a \mid T \geq T_L, (T_L, \mathbf{Z}, \mathbf{X}(T_L)) \in l_{\mathcal{T}}(a, \mathbf{z}, \mathbf{x})). \quad (3.1)$$

The probability $S_{\mathcal{T}}(t \mid a, \mathbf{z}, \mathbf{x})$ approximates the target function $S(t \mid a, \mathbf{z}, \mathbf{x})$.

3.2 Partition-based estimation at the landmark time

In the CFFPR data and many other applications, the follow-up of a subject can be terminated due to loss to follow-up or study end. We now consider estimating $S_{\mathcal{T}}(t \mid a, \mathbf{z}, \mathbf{x})$ with censored data. Denote by C the censoring time and assume that C is independent of (T_L, T, \mathbf{X}) given \mathbf{Z} . We follow the convention to define $Y = \min(T, C)$ and $\Delta = I(T \leq C)$. At the landmark time T_L , we further define $Y_L = \min(T_L, C)$ and $\Delta_L = I(T_L \leq T, T_L \leq C)$. Note that $\Delta_L = 1$ is the at-risk indicator at T_L . For subjects who are free of the failure event at T_L (i.e., $T \geq T_L$), one can observe T_L and $\mathbf{X}(T_L)$ when $\Delta_L = 1$ (i.e., $T_L \leq C$). The training data are $\{(Y_i, \Delta_i, Y_{Li}, \Delta_{Li}, \mathbf{X}_i(Y_{Li}), \mathbf{Z}_i), i = 1, \dots, n\}$, which are assumed to be independent identically distributed replicates of $(Y, \Delta, Y_L, \Delta_L, \mathbf{X}(Y_L), \mathbf{Z})$.

Define $N(t, a) = \Delta I(Y - a \leq t)$. Denote by $\lambda(t \mid a, \mathbf{z}, \mathbf{x})$ the landmark hazard function, that is, $\lambda(t \mid a, \mathbf{z}, \mathbf{x})dt = P(T - T_L \in [t, t + dt) \mid T - T_L \geq t, T_L = a, \mathbf{Z} = \mathbf{z}, \mathbf{X}(T_L) = \mathbf{x})$. The survival

function $S(t | a, \mathbf{z}, \mathbf{x})$ and the hazard function $\lambda(t | a, \mathbf{z}, \mathbf{x})$ have a one-to-one correspondence relationship: $S(t | a, \mathbf{z}, \mathbf{x}) = \exp\{-\int_0^t \lambda(u | a, \mathbf{z}, \mathbf{x})du\}$. For $t > 0$, we have

$$\begin{aligned}
& E\{N(dt, Y_L) - I(Y - Y_L \geq t)\lambda(t | a, \mathbf{z}, \mathbf{x})dt | \Delta_L = 1, Y_L = a, \mathbf{Z} = \mathbf{z}, \mathbf{X}(Y_L) = \mathbf{x}\} \\
&= E\{N(dt, a) - I(T \geq a + t, C \geq a + t)\lambda(t | a, \mathbf{z}, \mathbf{x})dt | C \geq a, T \geq T_L = a, \mathbf{Z} = \mathbf{z}, \mathbf{X}(T_L) = \mathbf{x}\} \\
&= E\{I(T - T_L \in [t, t + dt)) - I(T - T_L \geq t)\lambda(t | a, \mathbf{z}, \mathbf{x})dt | C \geq a, T \geq T_L = a, \mathbf{Z} = \mathbf{z}, \mathbf{X}(T_L) = \mathbf{x}\} \\
&\quad \times P(C \geq a + t | C \geq a, \mathbf{Z} = \mathbf{z}) \\
&= 0.
\end{aligned}$$

Then we have

$$\lambda(t | a, \mathbf{z}, \mathbf{x})dt = \frac{E\{N(dt, Y_L) | \Delta_L = 1, Y_L = a, \mathbf{Z} = \mathbf{z}, \mathbf{X}(Y_L) = \mathbf{x}\}}{E\{I(Y - Y_L \geq t) | \Delta_L = 1, Y_L = a, \mathbf{Z} = \mathbf{z}, \mathbf{X}(Y_L) = \mathbf{x}\}}. \quad (3.2)$$

Conditioning on $\Delta_L = 1$ and $(Y_L, \mathbf{Z}, \mathbf{X}(Y_L))$, subjects with $Y - Y_L \geq t$ can be viewed as a representative sample of the population with $T - T_L \geq t$ for each $t > 0$. Heuristically, the numerator and denominator in (3.2) can be estimated using partition-based estimators in the subsample with $\Delta_L = 1$. Given a partition \mathcal{T} , the function $S_{\mathcal{T}}(t | a, \mathbf{z}, \mathbf{x})$ in (3.1) can be estimated by the following estimator,

$$\widehat{S}_{\mathcal{T}}(t | a, \mathbf{z}, \mathbf{x}) = \exp \left\{ - \int_0^t \frac{\sum_{i=1}^n \Delta_{Li} I((Y_{Li}, \mathbf{Z}_i, \mathbf{X}_i(Y_{Li})) \in l_{\mathcal{T}}(a, \mathbf{z}, \mathbf{x})) N_i(du, Y_{Li})}{\sum_{i=1}^n \Delta_{Li} I((Y_{Li}, \mathbf{Z}_i, \mathbf{X}_i(Y_{Li})) \in l_{\mathcal{T}}(a, \mathbf{z}, \mathbf{x}), Y_i - Y_{Li} \geq u)} \right\}. \quad (3.3)$$

When a new subject is event-free at the landmark time T_{L0} with predictors \mathbf{Z}_0 and $\mathbf{X}_0(T_{L0})$, the predicted survival probability based on a single tree is $\widehat{S}_{\mathcal{T}}(t | T_{L0}, \mathbf{Z}_0, \mathbf{X}_0(T_{L0}))$. In practice, the partition \mathcal{T} can be constructed via a recursive partition algorithm based on the log-rank splitting rule (Ciampi et al., 1986; Segal, 1988), and the split-complexity pruning can be applied to determine the size of the tree (LeBlanc and Crowley, 1993).

3.3 Survival tree ensembles based on martingale estimating equations

It has been well-recognized that the prediction based on a single tree is often unstable. Ensemble methods such as bagging (Breiman, 1996) and random forests (Breiman, 2001) have been commonly applied to improve the prediction performance of classification and regression trees. The original random forests perform the prediction for a new data point by averaging predictions from a large number of trees, which are often grown sufficiently deep to achieve low bias (Friedman et al., 2001).

However, for censored data, a large tree may result in a small number of observed failures in the terminal nodes, leading to increased estimation bias of survival or cumulative hazard functions. Existing survival forest methods inherit from the original random forest and directly average the survival prediction from individual trees. Therefore, the node size parameter often needs to be carefully tuned to achieve good prediction accuracy. On the other hand, if the target estimate can be expressed as the solution of an unbiased estimating equation, a more natural way is to solve the averaged estimating equations from individual trees. In what follows, we propose an ensemble procedure based on averaging martingale estimating equations.

For $b = 1, \dots, B$, we draw the b th bootstrap sample from the training data. Let $\mathbb{T} = \{\mathcal{T}_b\}_{b=1}^B$ be a collection of B partitions constructed using the bootstrap datasets. Each partition is constructed via a recursive partition procedure where at each split, m ($m < p$) predictors are randomly selected as the candidate variables for splitting. Let l_b be the partition function based on the partition \mathcal{T}_b . The tree-based estimation from \mathcal{T}_b can be obtained from the following estimating equation,

$$\sum_{i=1}^n w_{bi} I((Y_{Li}, \mathbf{Z}_i, \mathbf{X}_i(Y_{Li})) \in l_b(a, \mathbf{z}, \mathbf{x})) \Delta_{Li} \{N_i(dt, Y_{Li}) - I(Y_i - Y_{Li} \geq t) \lambda(t | a, \mathbf{z}, \mathbf{x}) dt\} = 0,$$

where w_{bi} is the frequency of the i th observation in the b th bootstrap sample. Note that when $w_{bi} = 1$ for all $i = 1, \dots, n$, solving the above estimating equation yields the estimator in (3.3). To perform prediction using all the trees, we consider the following averaged estimating equation,

$$\sum_{i=1}^n w_i(a, \mathbf{z}, \mathbf{x}) \Delta_{Li} \{N_i(dt, Y_{Li}) - I(Y_i - Y_{Li} \geq t) \lambda(t | a, \mathbf{z}, \mathbf{x}) dt\} = 0,$$

where $w_i(a, \mathbf{z}, \mathbf{x}) = \sum_{b=1}^B w_{bi} I\{(Y_{Li}, \mathbf{Z}_i, \mathbf{X}_i(Y_{Li})) \in l_b(a, \mathbf{z}, \mathbf{x})\} / B$. Solving the averaged estimating equation yields

$$\widehat{S}_{\mathbb{T}}(t | a, \mathbf{z}, \mathbf{x}) = \exp \left\{ - \int_0^t \frac{\sum_{i=1}^n w_i(a, \mathbf{z}, \mathbf{x}) \Delta_{Li} N_i(ds, Y_{Li})}{\sum_{i=1}^n w_i(a, \mathbf{z}, \mathbf{x}) \Delta_{Li} I(Y_i - Y_{Li} \geq s)} \right\}.$$

The estimator $\widehat{S}_{\mathbb{T}}(t | a, \mathbf{z}, \mathbf{x})$ can be viewed as an adaptive nearest neighbour estimator (Lin and Jeon, 2006), where the weight assigned to each observation comes from random forests.

4 Evaluating the landmark prediction performance

The time-dependent receiver operating characteristics (ROC) curve is a popular tool in evaluating the capability of a marker in risk prediction. To evaluate the performance of the predicted risk score,

we extend the cumulative/dynamic ROC curves (Heagerty et al., 2000), which has been commonly used when a risk score is based on baseline predictors. For $t > 0$, subjects with $0 \leq T - T_L < t$ are considered as cases and subjects with $T - T_L \geq t$ are considered as controls. The ROC curve then evaluates the performance of a risk score that discriminates between subjects who have experienced the events prior to $T_L + t$ and those who do not.

Let $g(t, T_L, \mathbf{Z}, \mathbf{X}(T_L))$ denote a risk score based on $(T_L, \mathbf{Z}, \mathbf{X}(T_L))$, with a smaller value indicating a lower chance of $T - T_L \geq t$. For each t , The false positive rate and true positive rate at a threshold of c are defined as follows,

$$\text{FPR}(c) = P(g(t, T_L, \mathbf{Z}, \mathbf{X}(T_L)) > c \mid 0 \leq T - T_L < t),$$

$$\text{TPR}(c) = P(g(t, T_L, \mathbf{Z}, \mathbf{X}(T_L)) > c \mid T - T_L \geq t).$$

The ROC curve is defined as $\text{ROC}_t(p) = \text{TPR}(\text{FPR}^{-1}(p))$. Following the arguments of McIntosh and Pepe (2002), it can be shown that $g(t, a, \mathbf{z}, \mathbf{x}) = S(t \mid a, \mathbf{z}, \mathbf{x})$ yields the highest ROC curve, which justifies the use of the proposed time-dependent ROC curve. Moreover, the area under the ROC curve of $g(t, T_L, \mathbf{Z}, \mathbf{X}(T_L))$ is equivalent to the following concordance measure,

$$\begin{aligned} \text{CON}_t(g) = & P(g(t, T_{L1}, \mathbf{Z}, \mathbf{X}_1(T_{L1})) > g(t, T_{L2}, \mathbf{Z}, \mathbf{X}_2(T_{L2})) \mid 0 \leq T_2 - T_{L2} < t \leq T_1 - T_{L1}) + \\ & 0.5P(g(t, T_{L1}, \mathbf{Z}, \mathbf{X}_1(T_{L1})) = g(t, T_{L2}, \mathbf{Z}, \mathbf{X}_2(T_{L2})) \mid 0 \leq T_2 - T_{L2} < t \leq T_1 - T_{L1}), \end{aligned}$$

where $(T_{L1}, \mathbf{Z}_1, \mathbf{X}_1(T_{L1}), T_1)$ and $(T_{L2}, \mathbf{Z}_2, \mathbf{X}_2(T_{L2}), T_2)$ are independent pairs of observations, and the second term accounts for potential ties in the risk score.

In practice, one usually builds the model on a training dataset and evaluates its performance on an independent test dataset that are also subject to right censoring. To simplify notation here, we construct the estimator for $\text{CON}_t(g)$ using the observed data introduced in Section 3.2, although CON_t evaluated using the test data should be used in real applications. Define $d_{ij}(t) = g(t, Y_{Li}, \mathbf{Z}_i, \mathbf{X}_i(Y_{Li})) - g(t, Y_{Lj}, \mathbf{Z}_j, \mathbf{X}_j(Y_{Lj}))$. The $\text{CON}_t(g)$ measure can be consistently estimated by

$$\begin{aligned} \widehat{\text{CON}}_t(g) & \tag{4.1} \\ = & \frac{\sum_{i \neq j} \Delta_j \{I(d_{ij}(t) > 0) + 0.5I(d_{ij}(t) = 0)\} I(Y_j - Y_{Lj} \leq t < Y_i - Y_{Li}) / \widehat{S}_C(Y_j \mid \mathbf{Z}_j) \widehat{S}_C(Y_{Li} + t \mid \mathbf{Z}_i)}{\sum_{i \neq j} \Delta_j I(Y_j - Y_{Lj} \leq t < Y_i - Y_{Li}) / \widehat{S}_C(Y_j \mid \mathbf{Z}_j) \widehat{S}_C(Y_{Li} + t \mid \mathbf{Z}_i)}, \end{aligned}$$

where $\widehat{S}_C(t \mid \mathbf{z})$ is an estimator for the conditional censoring distribution $S_C(t \mid \mathbf{z}) = P(C \geq t \mid \mathbf{Z} = \mathbf{z})$. For example, existing survival tree or forest methods can be applied to estimate $S_C(t \mid \mathbf{z})$;

when censoring is completely random, the Kaplan-Meier estimator can also be applied. In practice, one can either use the concordance at a given time point t or an integrated measure to evaluate the overall concordance on a given time interval $[t_L, t_U]$. In the latter case, a weighted average of concordance on a grid of time points in $[t_L, t_U]$ can be reported.

5 Permutation variable importance

Variable importance is a useful measure for understanding the impact of predictors in tree ensembles and can be used as a reference for variable selection (Breiman, 2001). In the original random forests, each tree is constructed using a bootstrap sample of the original data, and the out-of-bag (OOB) data can be used to estimate the OOB prediction performance. The permutation variable importance of a predictor is computed as the average decrease in model accuracy on the OOB samples when the respective feature values are randomly permuted.

To study variable importance in dynamic risk prediction using censored data, we consider an extension of variable importance. Following the original random forests, the OOB prediction for each training observation is made based on trees constructed without using this observation. Applying the same arguments as in Section 4, the OOB survival prediction is obtained via the weighted estimating equations. Therefore, for the i th subject, the ensemble prediction using the trees built without the i th observation is

$$\widehat{S}_{-i}(t \mid a, \mathbf{z}, \mathbf{x}) = \exp \left\{ - \int_0^t \frac{\sum_{k=1}^n w_{k,-i}(a, \mathbf{z}, \mathbf{x}) dN_k(s, Y_{Lk})}{\sum_{k=1}^n w_{k,-i}(a, \mathbf{z}, \mathbf{x}) I(Y_k - Y_{Lk} \geq s)} \right\},$$

where $w_{k,-i}(a, \mathbf{z}, \mathbf{x}) = \sum_{b=1}^B w_{bk} I((Y_{Lk}, \mathbf{Z}_k, \mathbf{X}_k(Y_{Lk})) \in l_b(a, \mathbf{z}, \mathbf{x}), w_{bi} = 0) / \sum_{b=1}^B I(w_{bi} = 0)$. Define $d_{ij}(t) = \widehat{S}_{-i}(t \mid Y_{Li}, \mathbf{Z}_i, \mathbf{X}_i(Y_{Li})) - \widehat{S}_{-j}(t \mid Y_{Lj}, \mathbf{Z}_j, \mathbf{X}_j(Y_{Lj}))$. The OOB concordance at t can be calculated by applying (4.1).

To compute the permutation variable importance, we permute the values of predictors in $(Y_L, \mathbf{Z}, \mathbf{X}(Y_L))$ among subjects with $\Delta_L = 1$. In practice, one can either permute a single feature or permute a set of features, such as all the repeated measurements of a longitudinal marker, to understand its overall impact. We calculate the OOB concordance after permutation with $\widehat{S}_{-i}(t \mid Y_{Li}, \mathbf{Z}_i, \mathbf{X}_i(Y_{Li}))$ replaced by $\widehat{S}_{-i}(t \mid Y_{Li}^*, \mathbf{Z}_i^*, \mathbf{X}_i^*(Y_{Li}^*))$, where “*” is used to denote the predictors after permutation. As the permutation importance involves randomness in shuffling the predictors, we repeat the permutation multiple times and take the average difference in OOB

concordances over all the permutations.

6 Simulation

Simulation studies were conducted to assess the performance of the proposed methods. The time-independent predictors $\mathbf{Z} = \{Z_1, \dots, Z_{10}\}$ were generated from a multivariate normal distribution with $E(Z_i) = 1$, $\text{Var}(Z_i) = 1$, and $\text{Cov}(Z_i, Z_j) = 0.5^{|i-j|}$, for $i, j = 1, \dots, 10$. The longitudinal predictors $\mathbf{W}(t) = \{W_1(t), \dots, W_{10}(t)\}$ were generated from $W_i(t) = a_i F(b_i t)/t$, $i = 1, \dots, 10$, where a_i follows a uniform distribution on $[-1, 1]$, b_i follows a uniform distribution on $[0, 1]$, and $F(x) = 1 - \exp(-x^2)$. The longitudinal predictors were observed intermittently at certain time points as specified below. Two data generating mechanisms that mimic commonly encountered longitudinal studies were used in our simulations.

We first considered a scenario where the time-dependent predictors $\mathbf{W}(t)$ are regularly measured at fixed time points, t_1, \dots, t_K , where t_k serves as a landmark time. We are interested in predicting the event risk on the time interval (t_k, t_{k+1}) using predictors observed up to t_k , that is, $P\{T \geq t_k + t \mid T \geq t_k, \mathbf{W}(t_1), \dots, \mathbf{W}(t_k), \mathbf{Z}\}$ for $0 < t < t_{k+1} - t_k$ and $k \geq 1$. The failure time T was generated based on the following hazard function,

$$\lambda(t \mid \mathbf{W}(t), \mathbf{Z}) = 1.6I(t > 1) + 0.5 \exp \left\{ \sum_{j=1}^5 W_j(t) - \sum_{j=5}^9 Z_j + \sum_{j=1}^5 W_j(t) Z_{j+4} \right\}.$$

With these configurations, the median failure time is 1.51 when there is no censoring. Two fixed landmark time points at $t_1 = 1$ and $t_2 = 2$ were considered.

In the second scenario, we considered a multi-state model with three states: healthy, diseased, and death. We assume that all subjects started in the healthy state and all states were irreversible, so that only the transition paths health \rightarrow diseased \rightarrow death and health \rightarrow death are allowed. In this scenario, death is the event of interest and disease onset is an intermediate event. To simulate the data, we first generated an event time, D , from the accelerated failure time model,

$$\log D = -1 + \sum_{p=5}^9 Z_p + \gamma + \epsilon_1,$$

where ϵ_1 is a standard normal random variable and the frailty variable γ follows a gamma distribution with mean 1 and variance 0.5. Define the disease indicator, Π , where $\Pi = 1$ indicates

the subject moves from the healthy state to the disease state at time D , and $\Pi = 0$ indicates the subject moves from the healthy state to death at time D . The disease indicator was obtained via the following model:

$$\text{logit}\{P\{\Pi = 1 \mid \mathbf{Z}, \mathbf{W}(D)\}\} = 1 + \sum_{p=1}^5 W_p(D) + \sum_{p=5}^9 Z_p + \gamma.$$

Given a subject had developed the disease at time D , the residual survival time, R , was generated from

$$\log R = -1 + \sum_{p=1}^5 W_p(D) + \sum_{p=5}^9 Z_p + \sum_{p=1}^5 W_p(D)Z_{p+4} - \log(1 + D) + \gamma + \epsilon_2,$$

where ϵ_2 is a standard normal random variable. When $\Pi = 1$, the time to death is $T = D + R$ and the time to the intermediate event is $U = D$; when $\Pi = 0$, the time to death is $T = D$ and the intermediate event does not occur. When there is no censoring, the median failure time is 2.25 and about 85% of the subjects developed the disease before death. Motivated by the CFFPR data, we consider the situation where the landmark is the intermediate event and $\mathbf{W}(\cdot)$ is observed intermittently at $t_k = k$ for $k \geq 1$. The available predictors at the landmark time are then $\{U, \mathbf{W}(t_1, U), \dots, \mathbf{W}(t_K, U), \mathbf{Z}\}$, and the probability of interest is $P\{T \geq U + t \mid T \geq U, U, \mathbf{W}(t_1, U), \dots, \mathbf{W}(t_K, U), \mathbf{Z}\}$. In other applications, $\mathbf{W}(\cdot)$ can be observed at the intermediate event. For example, in electronic health records data, patients are observed at disease diagnosis and thus the marker measurements are recorded. In this case, we considered both a fixed landmark time and a random landmark time of disease onset. At a fixed landmark time point a , $\mathbf{W}(U)$ is observed only if $U \leq a$. Then the probabilities of interest are $P\{T - a \geq t \mid T \geq a, U, \mathbf{W}(U), \mathbf{Z}\}$ if $U \leq a$ and $P\{T - a \geq t \mid T \geq a, U > a, \mathbf{Z}\}$ otherwise. When the landmark time is U , $\mathbf{W}(U)$ is available for all subjects in the risk set, and the probability of interest is $P\{T \geq U + t \mid T \geq U, U, \mathbf{W}(U), \mathbf{Z}\}$.

For all scenarios, the censoring time was generated from a uniform distribution on $(0, c)$, where c was chosen to achieve either a 20% or 40% rate of censoring. We simulated 1000 training datasets with sample sizes of 200 and 400 at baseline. The trees were constructed with a minimum terminal node size of 15. When a single tree was used for prediction, the size of the tree was determined by split-complexity pruning via ten-fold cross-validation. To grow the trees in the ensemble method, we randomly selected $\lceil \sqrt{p} \rceil$ variables at each splitting step and did not prune the trees. Each fitted model was evaluated on independent test data with 500 observations. The evaluating criteria were the integrated concordance and the integrated mean squared error on the

interval $[0, t_0]$. The integrated mean squared error is defined as $\sum_{i=1}^{500} \int_0^{t_0} \{\widehat{S}(t | T_{Li}^0, \mathbf{Z}_i^0, \mathbf{X}_i^0(T_{Li}^0)) - S(t | T_{Li}^0, \mathbf{Z}_i^0, \mathbf{X}_i^0(T_{Li}^0))\}^2 dt / 500$, where the superscript 0 is used to denote the test data and t_0 is set to be approximately the 90% quantile of Y . For comparison, we also applied the landmark Cox models. In the first scenario, the predictors in the landmark Cox model are $\{\mathbf{W}(t_1), \dots, \mathbf{W}(t_k), \mathbf{Z}\}$ when the landmark time is t_k . In the second scenario, however, the number of available predictors depend on the landmark time as well as when $\mathbf{W}(\cdot)$ are measured. When the landmark time is U and $\mathbf{W}(\cdot)$ are measured at t_k , the predictors in the landmark Cox model are $\{U, \mathbf{Z}, \mathbf{W}(t_k)I(t_k \leq U), I(t_k > U); k \geq 1\}$. When the landmark time is fixed at a and $\mathbf{W}(\cdot)$ are observed at U , the predictors in the landmark Cox model are $\{\mathbf{Z}, UI(U \leq a), \mathbf{W}(U)I(U \leq a), I(a > U)\}$.

The simulation results are summarized in Table 1. The proposed ensemble method yields the smallest mean squared errors and the highest concordance for all scenarios considered. As the sample size increases, the mean squared error of the proposed methods decreases, and the integrated concordance slightly increases as it is expected to converge to the maximum value when true survival function is used. Our simulation shows that there is no clear advantage between a single-tree model and the Cox model except for the scenario under the multi-state model with $\mathbf{W}(t)$ are measured repeatedly. When comparing the tree model with the Cox model, we observe that a small mean squared error does not necessarily accompany by a large integrated concordance. We conjecture this is due to the fact that the concordance measure only depends on the order of the predicted survival probability and is less sensitive than the mean squared error in terms of risk calibration. In summary, the proposed ensemble method has strong performances and serves as an appealing tool for dynamic risk prediction.

7 Application to the Cystic Fibrosis Foundation Patient Registry Data

Understanding the risk factors associated with the progressive loss of lung function is crucial in managing CF. Prior studies of the Cystic Fibrosis Foundation Patient Registry (CFFPR) data have made significant impacts on the guideline of clinical management, leading to improved outcomes in CF patients over time. Still, a large proportion of premature mortality results directly or indirectly from the loss of lung function. The risk for lung disease depends on patient characteristics,

Table 1: Summaries of integrated mean squared error ($\times 1000$) and integrated concordance of different methods

T_L	n	censor%	Integrated mean squared error			Integrated concordance		
			Tree	Ensemble	Cox	Tree	Ensemble	Cox
Scenario 1								
$t_1 = 1$	200	20%	25.002	5.708	27.655	0.535	0.585	0.527
		40%	22.354	5.664	29.845	0.536	0.587	0.528
	400	20%	18.313	4.678	13.306	0.538	0.592	0.534
		40%	15.663	4.804	14.553	0.538	0.591	0.535
$t_2 = 2$	200	20%	25.217	5.782	25.944	0.523	0.574	0.515
		40%	21.819	5.762	29.415	0.523	0.571	0.512
	400	20%	18.222	4.645	13.313	0.529	0.592	0.523
		40%	14.597	4.964	14.211	0.526	0.579	0.522
Scenario 2								
$\mathbf{W}(t)$ is measured at t_1, t_2, \dots, t_K								
U	200	20%	85.486	63.100	318.931	0.648	0.745	0.522
		40%	86.699	61.201	322.366	0.614	0.711	0.533
	400	20%	80.612	63.188	319.935	0.671	0.767	0.544
		40%	80.119	58.880	325.754	0.651	0.742	0.544
$\mathbf{W}(t)$ is measured at U								
$t_2 = 2$	200	20%	58.274	24.728	58.041	0.718	0.742	0.717
		40%	61.000	21.877	68.021	0.681	0.750	0.689
	400	20%	42.140	23.660	49.361	0.681	0.753	0.741
		40%	48.739	19.789	58.289	0.689	0.776	0.732
U	200	20%	54.212	36.033	50.325	0.603	0.661	0.632
		40%	53.469	34.762	53.971	0.618	0.688	0.688
	400	20%	51.118	30.101	41.782	0.626	0.692	0.638
		40%	50.061	28.809	40.629	0.629	0.704	0.685

and certain patient groups, such as Hispanic patients, are at increased risk of severe disease for reasons not yet known (McGarry et al., 2019). Our goal is to build a prediction algorithm for the development of moderate airflow limitation, defined as the first time that ppFEV1 drops below 80% in CFPPR. The data consist of 5,398 pediatric CF patients who were diagnosed before one year of age between 2008 and 2013; among them, 419 were Hispanic. In our analysis, the data were subjected to right-censoring due to loss of follow-up or administrative censoring. A total of 4,507 failure events were observed with a median follow-up time of 7.71 years. The median age of event occurrence derived from the Kaplan-Meier estimate was 7.95 years (95% confidence interval, 7.81–8.16).

The rich information in the CFPPR data renders the possibility of a comprehensive evaluation of important risk factors. We considered baseline predictors including gender (female vs. male), ethnicity (Hispanic vs. non-Hispanic), maternal education status (≥ 16 years of education vs. else), insurance status at enrollment (insured vs. not insured), geographic location (West, Midwest, Northeast, and South), and mutation class (severe, mild, and unknown). Since baseline factors usually have limited predictability in longitudinal follow-up studies like CFPPR, we further included repeated measurements and intermediate events as predictors. The longitudinal measurements, ppFEV1, percent predicted forced vital capacity (ppFVC), weight, and height, were assessed regularly throughout the study and were annualized at integer ages via linear interpolation. The intermediate events include different subtypes of PA (initial acquisition, mucoid, chronic, multidrug-resistant), methicillin-sensitive staphylococcus aureus (MSSA), methicillin-resistant staphylococcus aureus (MRSA), as well as the diagnoses of CF-related diabetes (CFRD) and pancreatic insufficiency.

For landmark prediction, we considered the following fixed and random landmark times:

- (LM1) The landmark time is age 7, with the target prediction interval [7, 22].
- (LM2) The landmark time is age 12, with the target prediction interval [12, 22].
- (LM3) The landmark time is the acquisition of chronic *Pseudomonas aeruginosa* (cPA), and the target prediction interval is from the time of acquiring cPA to age 22.

The fixed landmark ages 7 and 12 correspond to middle childhood and preadolescence. The random landmark event cPA was considered because it has been shown that patients with cPA are more

likely to develop increased inflammation, leading to an accelerated loss in lung function (Kamata et al., 2017). To perform risk prediction, we used Model (LM1) to obtain the future risk for a patient who is event-free at age 7. An updated prediction can be carried out using Model (LM2) if the patient remains event-free at age 12. Upon converting to cPA, patients who are clinically stable can become unstable, and the predicted risk can be updated using Model (LM3). To illustrate the event history and landmark times, we show the occurrence of PA during the follow-up period for a random sample of 50 patients in Figure 2. As time goes by, more information on the intermediate events becomes available. At each landmark time, the exact timing of an intermediate event is only available if it has occurred before the landmark time.

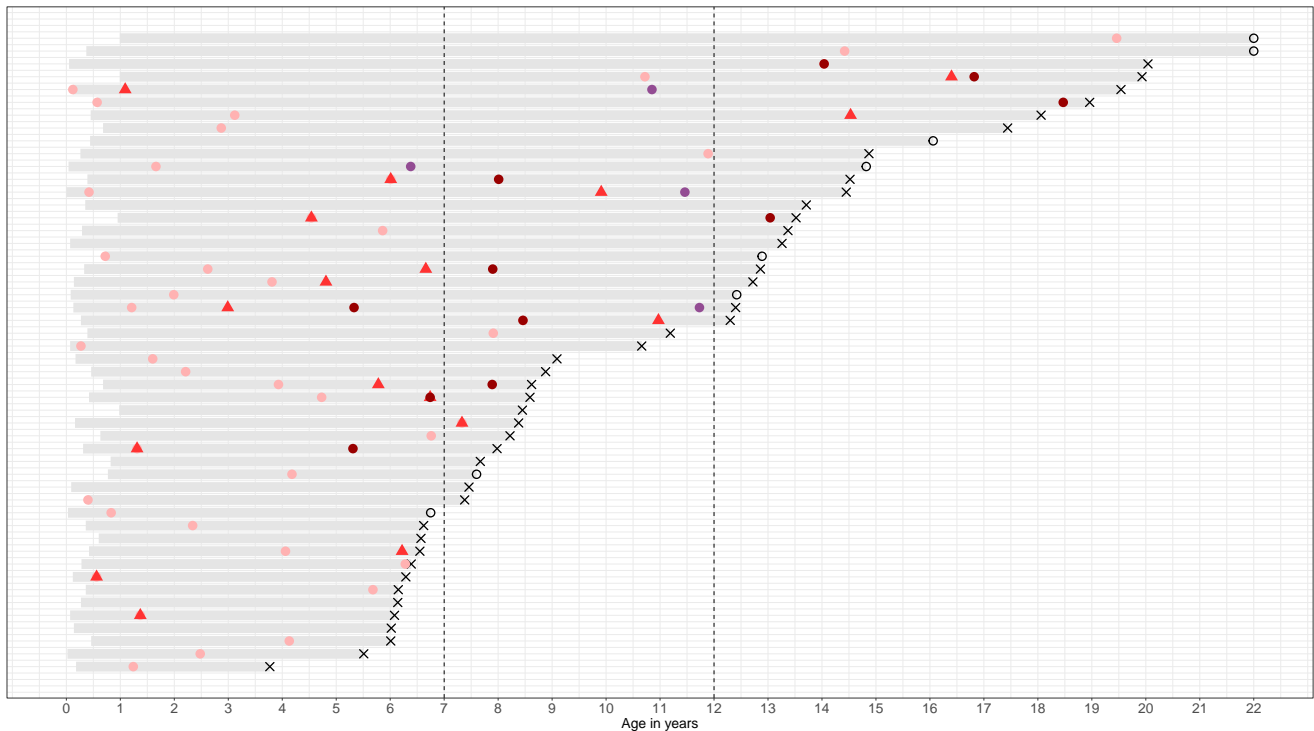


Figure 2: Illustration of the acquisition of different subtypes of PA from 50 random subjects in the CFFPR data. Each line corresponds to one subject. \times marks the failure event; \circ marks censoring; \bullet marks the initial PA; \blacktriangle marks the chronic PA, which serves as a random landmark in the Model (LM3); \bullet marks the mucoid PA; \bullet marks the multi-drug resistant PA. The two fixed landmark time points (ages 7 and 12) are marked by the vertical dashed lines.

The data were randomly partitioned into a training set (60%) and a test set (40%). The landmark prediction models were built using the training data, and their performances were evaluated

on the test data via the proposed concordance measure in Section 4. Results from landmark Cox models were also reported for comparison. Similar to the conventional landmark prediction models, a Cox model was constructed using subjects who remained event-free and uncensored at each landmark time. In the Cox models, the j th partially observed intermediate events was incorporated via two predictors, $U_j I(U_j \leq T_L)$ and $I(U_j > T_L)$; the partially observed repeated measurements at t_k were expressed using $\mathbf{W}(t_k) I(t_k \leq T_L)$ and $I(t_k > T_L)$ under Model (LM3). The models were built in the way described in the simulation section.

The concordance measures are summarized in Table 2. For landmark prediction at ages 7 and 12, we reported the average CON_t at 50 equally spaced time points on the target prediction intervals. For the prediction at the landmark age of 12, both Models (LM1) and (LM2) can be applied: (LM1) used history up to age 7 while (LM2) uses history up to age 12. As expected, incorporating additional information collected between ages 7 and 12 results in an increase of average concordance from 0.711 to 0.739 in our ensemble model. For the landmark model at cPA, we used the concordance at a time horizon of five years after cPA as the evaluation criterion. Since we focus on the event risk prior to age 22, predicting the 5-year risk for individuals who acquired the chronic form of PA after age 17 is not feasible. Therefore, the concordance was evaluated in the subsample of subjects who developed cPA before age 17. As expected, the ensemble method yields better prediction performances compared to its competitors.

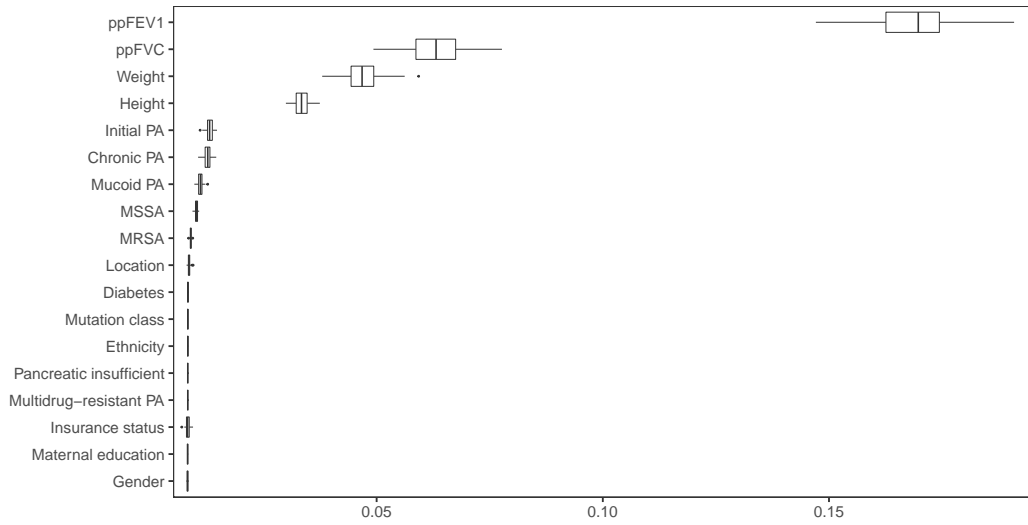
Landmark	Measure	Model	Tree	Ensemble	Cox
Age 7	$\widehat{\text{CON}}_{[0,15]}$	LM1	0.654	0.748	0.695
Age 12	$\widehat{\text{CON}}_{[0,10]}$	LM2	0.667	0.739	0.674
Age 12	$\widehat{\text{CON}}_{[0,10]}$	LM1	0.620	0.711	0.611
cPA	$\widehat{\text{CON}}_5$	LM3	0.763	0.813	0.788

Table 2: Concordance measures evaluated using the test data in the CFFPR analysis. The column Landmark gives the left bound of the target prediction interval. The integrated concordance is reported for Models (LM1) and (LM2) over the interval where the risk prediction is performed, where $\widehat{\text{CON}}_{[a,b]} = \sum_{j=1}^{50} \widehat{\text{CON}}_{t_j} / 50$ and $t_j = a + (b - a)j/50$. The concordance at year 5 after cPA is reported for Model (LM3).

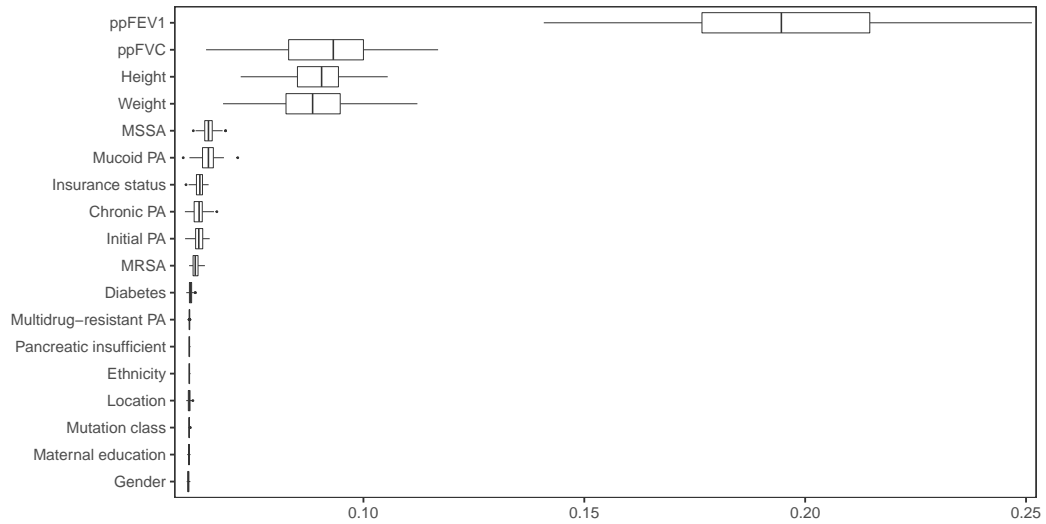
In an attempt to identify important predictors in the ensemble models, we computed the per-

mutation variable importance described in Section 5 with 100 permutations. Under the fixed landmark time models, we permuted all of the repeated measurements of a marker simultaneously to evaluate the overall impact of the longitudinal marker. The results of the permutation variable importance are summarized in Figure 3, where ppFEV1, ppFVC, weight, and height are identified as the top four important predictors for both landmark ages 7 and 12 (Figures 3A and 3B). Following them, intermediate events related to PA and staphylococcus aureus are moderately important. We note that mucoid PA and MSSA became more important at age 12 when compared to age 7. This could be due to the fact that these intermediate events are less common before age 7. When using cPA as the landmark, the longitudinal measurements after the acquisition of cPA were not used in prediction, and thus the number of observed repeated measurements varied across subjects. Unlike baseline variables and intermediate events of which the permutations were performed among subjects who experienced cPA, the permutation of a marker at a specific time point (e.g., age 7) was performed among subjects who experienced cPA after the time point. To this end, we plot the variable importance for predictors at different ages separately, so that the variable importance measures in each plot are based on permuting the same set of subjects. Figure 4A shows the importance of baseline variables and intermediate events, and the timing of cPA plays an important role in predicting future event risk. Figure 4B and Figure 4C show the importance of four longitudinal markers at ages 7 and 12, respectively.

Our models identify repeated measurements of weight and height as important variables in landmark prediction, which is consistent with the previous finding that malnutrition is a well-recognized adverse prognostic factor in CF (Konstan et al., 2003). To provide more insight into how historical weight measurements affect future risk in our ensemble model, we present the predicted event-free probabilities for hypothetical patients with different weight trajectories in Figure 5. Specifically, we consider Hispanic and non-Hispanic male patients whose weights were in the 10th, 50th, and 90th weight-for-age percentiles of the corresponding ethnicity-gender subgroup. For all six patients, the intermediate event times were fixed at the median derived from the Kaplan-Meier estimates, while categorical predictors and continuous predictors were fixed at the reference levels and mean values, respectively. At the landmark age 7, patients with the 10th percentile weight trajectories had the highest predicted risk, followed by patients with 90th percentile and those with 50th percentile weight trajectories (Figure 5A). This suggests a non-monotone relationship between weight and significant loss of lung function. At the landmark age 12, the predicted risk

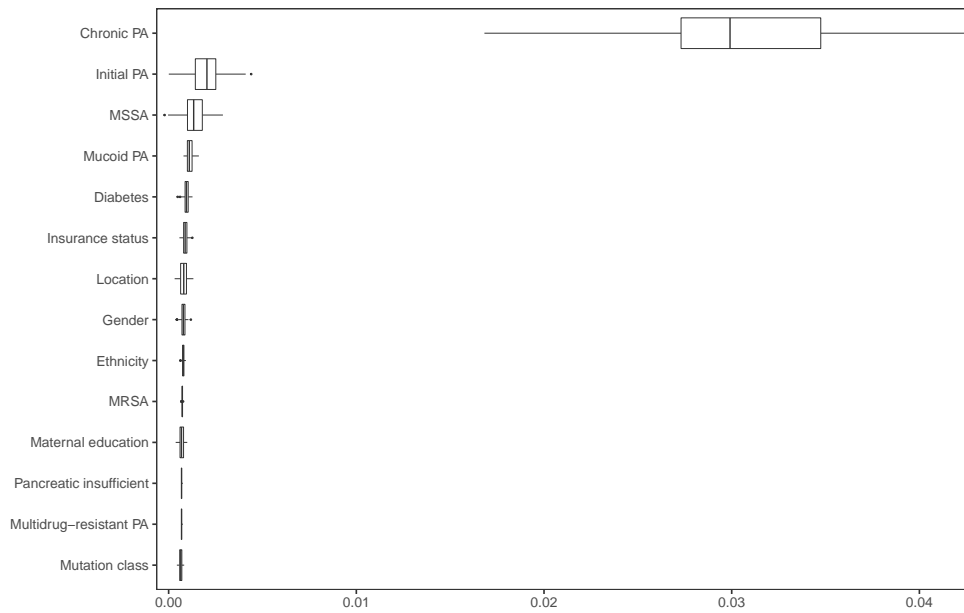


(A) Variable importance when the landmark time is age 7 and the risk prediction interval is $[7, 22]$.

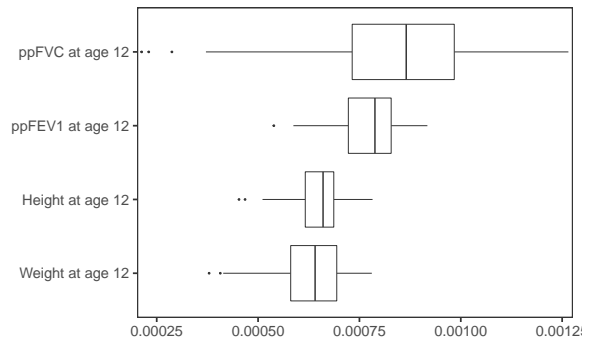
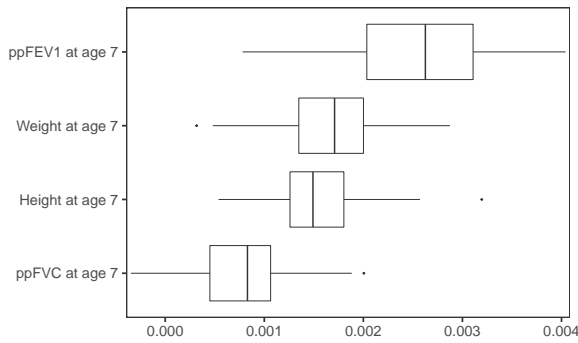


(B) Variable importance when the landmark time is age 12 and the risk prediction interval is $[12, 22]$.

Figure 3: The permutation variable importance in the CFFPR data analysis, when the landmark times are ages 7 and 12. The boxplots show the decreases in OOB concordances from the 100 permutations and are ranked in descending order according to the mean value.



(A) Variable importance for baseline variables and intermediate events

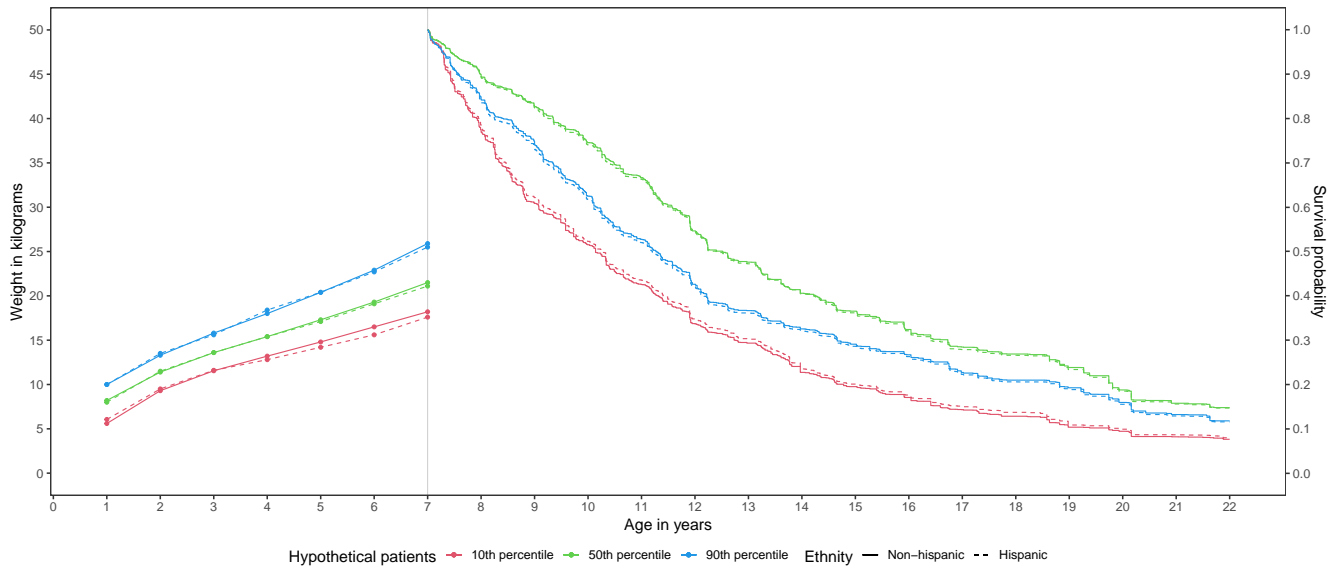


(B) Variable importance for markers at age 7. (C) Variable importance for markers at age 12.

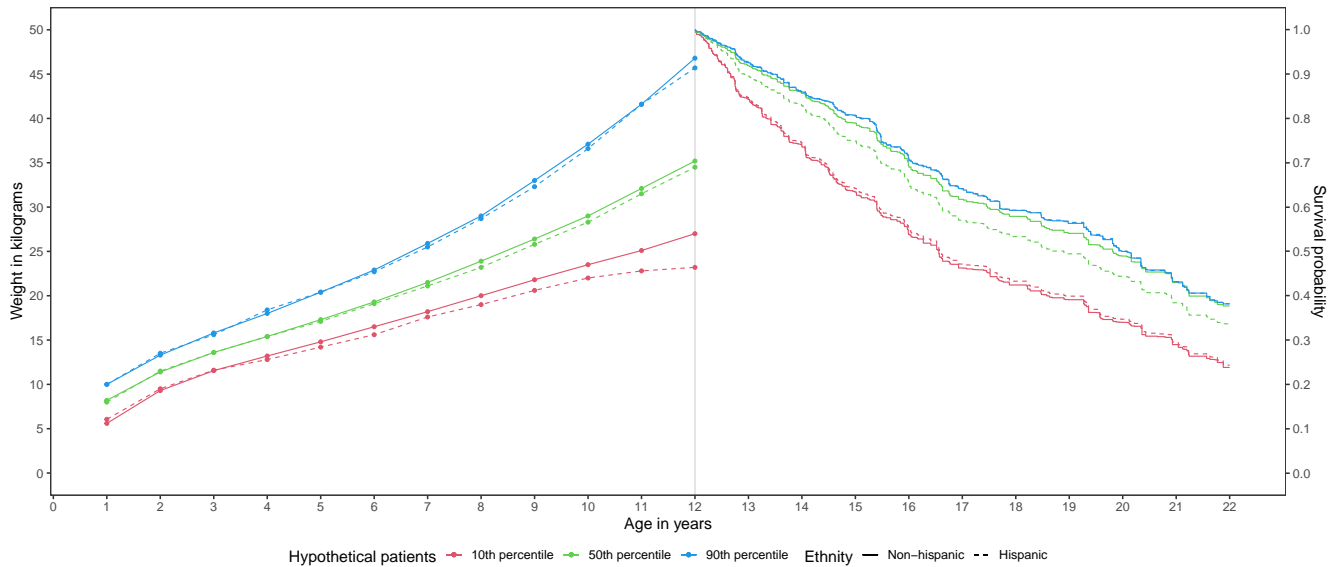
Figure 4: The permutation variable importance in the CFFPR data analysis, when the landmark time is cPA. The boxplots show the decreases in OOB concordances from the 100 permutations and are ranked in descending order according to the mean value.

in patients with 10th percentile weight remains the highest (Figure 5B). Interestingly, the non-Hispanic patient with the 90th percentile weight trajectory has a similar risk compared with his 50th percentile counterpart. On the other hand, the Hispanic patient with the 90th percentile weight trajectory has a lower risk than his 50th percentile counterpart.

It is worthwhile to point out that baseline factors such as ethnicity have a relatively low variable importance in the ensemble model. However, this does not mean that ethnicity does not affect



(A) Landmark time point at age 7, predicting the event risk on $[7, 22]$.



(B) Landmark time point at age 12, predicting the event risk on $[12, 22]$.

Figure 5: Survival predictions for patients in different weight groups. Curves on the left show the repeated weight measurements before the landmark time. Curves on the right show the survival predictions over the interval of interests for the corresponding groups. The weight groups were chosen by the percentiles and ethnicity, **—●—**: 10th percentile, non-Hispanic; **—●—**: 50th percentile, non-Hispanic; **—●—**: 90th percentile, non-Hispanic; **- -●- -**: 10th percentile, Hispanic; **- -●- -**: 50th percentile, Hispanic; **- -●- -**: 90th percentile, Hispanic.

the risk of lung function decline. We conjecture that the effect of ethnicity was predominantly mediated through spirometry measurements such as ppFEV1. Therefore, one should be cautious when interpreting the variable importance measure. When applying the proposed method in health disparity research, we recommend investigators to further build separate models for Hispanic and non-Hispanic patients to provide more insights into the heterogeneous populations and differences in risk of lung function decline. Additional analyses conducted in different ethnic groups are included in the Supplementary Materials.

8 Discussion

In this paper, we proposed a unified framework for event risk prediction with updated information using recursive partition and ensemble methods. Compared to semiparametric methods, the proposed methods can handle a large, growing number of predictors over time and are more robust to model misspecification. Furthermore, the landmark times at which a prediction is performed are allowed to be subject-specific and defined by intermediate clinical events. Notably, our ensemble procedure is based on averaging the unbiased martingale estimation equations instead of survival probabilities, thus avoids the potential bias arising due to small sizes in the terminal nodes.

The discussion in Section 2.1 has focused on the case where the time-dependent variables $\mathbf{W}(\cdot)$ are observed at fixed time points t_1, \dots, t_K . It is worthwhile to point out that the proposed method can also be applied to the case where repeated measures are taken at sparse, irregular time points. An important application is the analysis of electronic health record data, where lab tests are performed at medical encounters. Note that the medical encounters can be treated as intermediate events, of which the occurrence times are often predictive of the event risk. To see this, suppose $\mathbf{W}(\cdot)$ are observed at random time points (V_1, V_2, \dots, V_K) and the counting process for observation is $O(t) = \sum_{k=1}^K I(V_k \leq t)$. The history observed up to t is $\mathcal{H}_W(t) = \{\mathbf{W}(s)dO(s), I(V_k \leq s), 0 < s \leq t, k = 1, \dots, K\}$. At time t , the available information can be expressed using $\mathbf{X}(t) = \{\mathbf{W}(V_1, t), \dots, \mathbf{W}(V_K, t), V_1(t), \dots, V_K(t)\}$, where $V_k(t) = V_k$ if $V_k \leq t$ and $V_k(t) = t^+$ otherwise. In this way, the proposed method can be applied to construct the survival tree ensembles. Therefore, our framework can easily incorporate additional information observed at intermediate events and can deal with general electronic health record data.

Acknowledgements

The authors would like to thank the Cystic Fibrosis Foundation for the use of the CF Foundation Patient Registry data to conduct this study. Additionally, we would like to thank the patients, care providers, and care coordinators at CF centers throughout the United States for their contributions to the CF Foundation Patient Registry. The views expressed in this manuscript are those of the authors and do not necessarily represent the views of the National Heart, Lung and Blood Institute (NHLBI), the National Institutes of Health (NIH) and the U.S. Department of Health and Human Services. Colin O. Wu’s research was supported in part by the Intramural Research Program of the NHLBI/NIH. Chiung-Yu Huang’s research was supported by National Institutes of Health (NIH) (R01CA193888). Meghan McGarry’s research was supported by NIH (1K23HL133437-01A1) and Cystic Fibrosis Foundation Therapeutics (MCGARR16A0).

References

- Breiman, L. (1996), “Bagging Predictors,” *Machine learning*, 24, 123–140.
- (2001), “Random Forests,” *Machine Learning*, 45, 5–32.
- Ciampi, A., Thiffault, J., Nakache, J.-P., and Asselain, B. (1986), “Stratification by Stepwise Regression, Correspondence Analysis and Recursive Partition: A Comparison of Three Methods of Analysis for Survival Data with Covariates,” *Computational Statistics & Data Analysis*, 4, 185–204.
- Davis, R. B. and Anderson, J. R. (1989), “Exponential Survival Trees,” *Statistics in Medicine*, 8, 947–961.
- Domanski, M. J., Tian, X., Wu, C. O., Reis, J. P., Dey, A. K., Gu, Y., Zhao, L., Bae, S., Liu, K., Hasan, A. A., et al. (2020), “Time Course of LDL Cholesterol Exposure and Cardiovascular Disease Event Risk,” *Journal of the American College of Cardiology*, 76, 1507–1516.
- Friedman, J., Hastie, T., and Tibshirani, R. (2001), *The Elements of Statistical Learning*, New York: Springer.

- Gordon, L. and Olshen, R. A. (1985), “Tree-Structured Survival Analysis.” *Cancer Treatment Reports*, 69, 1065–1069.
- Heagerty, P. J., Lumley, T., and Pepe, M. S. (2000), “Time-Dependent ROC Curves for Censored Survival Data and a Diagnostic Marker,” *Biometrics*, 56, 337–344.
- Hothorn, T., Bühlmann, P., Dudoit, S., Molinaro, A., and Van Der Laan, M. J. (2006), “Survival Ensembles,” *Biostatistics*, 7, 355–373.
- Hothorn, T., Lausen, B., Benner, A., and Radespiel-Tröger, M. (2004), “Bagging Survival Trees,” *Statistics in Medicine*, 23, 77–91.
- Ishwaran, H., Kogalur, U. B., Blackstone, E. H., and Lauer, M. S. (2008), “Random Survival Forests,” *The Annals of Applied Statistics*, 2, 841–860.
- Jewell, N. P. and Nielsen, J. P. (1993), “A Framework for Consistent Prediction Rules Based on Markers,” *Biometrika*, 80, 153–164.
- Kamata, H., Asakura, T., Suzuki, S., Namkoong, H., Yagi, K., Funatsu, Y., Okamori, S., Uno, S., Uwamino, Y., Fujiwara, H., Nishimura, T., Ishii, M., Betsuyaku, T., and Hasegawa, N. (2017), “Impact of Chronic *Pseudomonas Aeruginosa* Infection on Health-Related Quality of Life in *Mycobacterium Avium* Complex Lung Disease,” *BMC Pulmonary Medicine*, 17, 198.
- Knapp, E. A., Fink, A. K., Goss, C. H., Sewall, A., Ostrenga, J., Dowd, C., Elbert, A., Petren, K. M., and Marshall, B. C. (2016), “The Cystic Fibrosis Foundation Patient Registry. Design and Methods of a National Observational Disease Registry,” *Annals of the American Thoracic Society*, 13, 1173–1179.
- Konstan, M. W., Butler, S. M., Wohl, M. E. B., Stoddard, M., Matousek, R., Wagener, J. S., Johnson, C. A., Morgan, W. J., and Investigators Coordinators of the Epidemiologic Study of Cystic Fibrosis (2003), “Growth and Nutritional Indexes in Early Life Predict Pulmonary Function in Cystic Fibrosis,” *The Journal of Pediatrics*, 142, 624–630.
- LeBlanc, M. and Crowley, J. (1992), “Relative Risk Trees for Censored Survival Data,” *Biometrics*, 48, 411–425.

- (1993), “Survival Trees by Goodness of Split,” *Journal of the American Statistical Association*, 88, 457–467.
- Li, L., Luo, S., Hu, B., and Greene, T. (2017), “Dynamic Prediction of Renal Failure Using Longitudinal Biomarkers in a Cohort Study of Chronic Kidney Disease,” *Statistics in Biosciences*, 9, 357–378.
- Lin, Y. and Jeon, Y. (2006), “Random Forests and Adaptive Nearest Neighbors,” *Journal of the American Statistical Association*, 101, 578–590.
- Mannino, D. M., Reichert, M. M., and Davis, K. J. (2006), “Lung Function Decline and Outcomes in an Adult Population,” *American Journal of Respiratory and Critical Care Medicine*, 173, 985–990.
- McGarry, M. E., Huang, C.-Y., Nielson, D., and Ly, N. P. (2020), “Early Acquisition and Conversion of *Pseudomonas Aeruginosa* in Hispanic Youth with Cystic Fibrosis in the United States,” *Journal of Cystic Fibrosis*, In press.
- McGarry, M. E., Neuhaus, J. M., Nielson, D. W., and Ly, N. P. (2019), “Regional Variations in Longitudinal Pulmonary Function: A Comparison of Hispanic and Non-Hispanic Subjects with Cystic Fibrosis in the United States,” *Pediatric Pulmonology*, 54, 1382–1390.
- McIntosh, M. W. and Pepe, M. S. (2002), “Combining Several Screening Tests: Optimality of the Risk Score,” *Biometrics*, 58, 657–664.
- Molinaro, A. M., Dudoit, S., and Van der Laan, M. J. (2004), “Tree-Based Multivariate Regression and Density Estimation with Right-Censored Data,” *Journal of Multivariate Analysis*, 90, 154–177.
- Morgan, W. J., Vandevanter, D. R., Pasta, D. J., Foreman, A. J., Wagener, J. S., Konstan, M. W., Morgan, W., Konstan, M., Liou, T., McColley, S., et al. (2016), “Forced Expiratory Volume in 1 Second Variability Helps Identify Patients with Cystic Fibrosis at Risk of Greater Loss of Lung Function,” *The Journal of Pediatrics*, 169, 116–121.

- Parast, L., Cheng, S.-C., and Cai, T. (2012), “Landmark Prediction of Long-Term Survival Incorporating Short-Term Event Time Information,” *Journal of the American Statistical Association*, 107, 1492–1501.
- Proust-Lima, C., Dartigues, J.-F., and Jacqmin-Gadda, H. (2016), “Joint Modeling of Repeated Multivariate Cognitive Measures and Competing Risks of Dementia and Death: A Latent Process and Latent Class Approach,” *Statistics in Medicine*, 35, 382–398.
- Rizopoulos, D. (2011), “Dynamic Predictions and Prospective Accuracy in Joint Models for Longitudinal and Time-To-Event Data,” *Biometrics*, 67, 819–829.
- Rizopoulos, D., Molenberghs, G., and Lesaffre, E. M. (2017), “Dynamic Predictions with Time-Dependent Covariates in Survival Analysis Using Joint Modeling and Landmarking,” *Biometrical Journal*, 59, 1261–1276.
- Segal, M. R. (1988), “Regression Trees for Censored Data,” *Biometrics*, 44, 35–47.
- Steingrimsson, J. A., Diao, L., Molinaro, A. M., and Strawderman, R. L. (2016), “Doubly Robust Survival Trees,” *Statistics in Medicine*, 35, 3595–3612.
- Steingrimsson, J. A., Diao, L., and Strawderman, R. L. (2019), “Censoring Unbiased Regression Trees and Ensembles,” *Journal of the American Statistical Association*, 114, 370–383.
- Taylor, J. M., Park, Y., Ankerst, D. P., Proust-Lima, C., Williams, S., Kestin, L., Bae, K., Pickles, T., and Sandler, H. (2013), “Real-Time Individual Predictions of Prostate Cancer Recurrence Using Joint Models,” *Biometrics*, 69, 206–213.
- van Houwelingen, H. C. (2007), “Dynamic Prediction by Landmarking in Event History Analysis,” *Scandinavian Journal of Statistics*, 34, 70–85.
- van Houwelingen, H. C. and Putter, H. (2008), “Dynamic Predicting by Landmarking as an Alternative for Multi-State Modeling: An Application to Acute Lymphoid Leukemia Data,” *Lifetime Data Analysis*, 14, 447–463.
- (2011), *Dynamic Prediction in Clinical Survival Analysis*, Boca Raton: CRC Press.

- Vidal-Petiot, E., Stebbins, A., Chiswell, K., Ardissino, D., Aylward, P. E., Cannon, C. P., Ramos Corrales, M. A., Held, C., López-Sendón, J. L., Stewart, R. A., et al. (2017), “Visit-To-Visit Variability of Blood Pressure and Cardiovascular Outcomes in Patients with Stable Coronary Heart Disease. Insights from the STABILITY Trial,” *European Heart Journal*, 38, 2813–2822.
- Wang, J., Luo, S., and Li, L. (2017), “Dynamic Prediction for Multiple Repeated Measures and Event Time Data: An Application to Parkinson’s Disease,” *The Annals of Applied Statistics*, 11, 1787–1809.
- Zhang, H. (1995), “Splitting Criteria in Survival Trees,” *Statistical Modelling*, 104, 305–313.
- Zhang, H., Holford, T., and Bracken, M. B. (1996), “A Tree-Based Method of Analysis for Prospective Studies,” *Statistics in Medicine*, 15, 37–49.
- Zhang, H. and Singer, B. H. (2010), *Recursive Partitioning and Applications*, New York: Springer.
- Zheng, Y. and Heagerty, P. J. (2005), “Partly Conditional Survival Models for Longitudinal Data,” *Biometrics*, 61, 379–391.
- Zhu, R. and Kosorok, M. R. (2012), “Recursively Imputed Survival Trees,” *Journal of the American Statistical Association*, 107, 331–340.
- Zhu, Y., Li, L., and Huang, X. (2019), “Landmark Linear Transformation Model for Dynamic Prediction with Application to a Longitudinal Cohort Study of Chronic Disease,” *Journal of the Royal Statistical Society: Series C (Applied Statistics)*, 68, 771–791.